Synthesis, characterization, and in vitro evaluation of the selective $P2Y_2$ receptor antagonist AR-C118925

Muhammad Rafehi [1,2] · Joachim C. Burbiel [1] · Isaac Y. Attah [1,2] · Aliaa Abdelrahman [1,2] · Christa E. Müller [1,2]

Abstract The G_q protein-coupled, ATP- and UTP-activated $P2Y_2$ receptor is a potential drug target for a range of different disorders, including tumor metastasis, inflammation, atherosclerosis, kidney disorders, and osteoporosis, but pharmacological studies are impeded by the limited availability of suitable antagonists. One of the most potent and selective antagonists is the thiouracil derivative AR-C118925. However, this compound was until recently not commercially available and little is known about its properties. We therefore developed an improved procedure for the synthesis of AR-C118925 and two derivatives to allow up-scaling and assessed their potency in calcium mobilization assays on the human and rat $P2Y_2$ receptors recombinantly expressed in 1321N1 astrocytoma cells. The compound was further evaluated for inhibition of $P2Y_2$ receptor-induced β-arrestin translocation. AR-C118925 behaved as a competitive antagonist with pA_2 values of 37.2 nM (calcium assay) and 51.3 nM (β-arrestin assay). Selectivity was assessed vs. related receptors including P2X, P2Y, and adenosine receptor subtypes, as well as ectonucleotidases. AR-C118925 showed at least 50-fold selectivity against the other investigated targets, except for the P2X1 and P2X3 receptors which were blocked by AR-C118925 at concentrations of about 1 μM. AR-C118925 is soluble in buffer at pH 7.4 (124 μM) and was found to be metabolically highly stable in human and mouse liver microsomes. In Caco2 cell experiments, the compound displayed moderate permeability indicating that it may show limited peroral bioavailability. AR-C118925 appears to be a useful pharmacological tool for in vitro and in vivo studies.

Keywords Antagonist · AR-C118925 · 1321N1 astrocytoma cells · G protein-coupled receptor · P2 receptor · $P2Y_2$ receptor · Synthesis · Thiouracil derivative

Abbreviations

AIBN	Azobisisobutyronitrile
AP_4A	Diadenosine tetraphosphate
AR-C118925	5-{[5-(2,8-Dimethyl-5*H*-dibenzo[a,d]cyclohepten-5-yl)-3,4-dihydro-2-oxo-4-thioxo-1(2*H*)-pyrimidinyl]methyl}-*N*-(1*H*-tetrazol-5-yl)-2-furancarboxamide
ATP	Adenosine-5′-triphosphate
CHO	Chinese hamster ovary
CYP	Cytochrome P450
DMEM	Dulbecco's modified Eagle's medium
DMF	Dimethylformamide
DMF-DEA	Dimethylformamide-diethylacetal
E5′-NT	Ecto-5′-nucleotidase
EDTA	Ethylenediaminetetraacetic acid
Fluo-4AM	Fluo-4 acetoxymethyl ester
MRS2768	Uridine-5′-tetraphosphate δ-phenyl ester tetrasodium salt
HBSS	Hank's balanced salt solution
HMDS	Hexamethyldisilazane
hNPP1	Human nucleotide pyrophosphatase subtype 1

Electronic supplementary material The online version of this article (doi:10.1007/s11302-016-9542-3) contains supplementary material, which is available to authorized users.

✉ Christa E. Müller
christa.mueller@uni-bonn.de

[1] PharmaCenter Bonn, Pharmaceutical Institute, Pharmaceutical Sciences Bonn (PSB), Pharmaceutical Chemistry I, University of Bonn, Bonn, Germany

[2] Pharmazeutisches Institut, Pharmazeutische Chemie I, An der Immenburg 4, D-53121 Bonn, Germany

hNTPDase2	Human nucleoside triphosphate diphosphohydrolase subtype 2
HOBt	Hydroxybenzotriazole
LDA	Lithium diisopropylamide
NBS	*N*-Bromosuccinimide
rt	Room temperature
SEM	Standard error of the mean
THF	Tetrahydrofuran
UTP	Uridine-5′-triphosphate
vs	Versus

Introduction

The P2Y nucleotide receptors are a family of G protein-coupled receptors that consists of eight mammalian subtypes. These are the $P2Y_1$-like receptors $P2Y_1$, $P2Y_2$, $P2Y_4$, $P2Y_6$, and $P2Y_{11}$, as well as the $P2Y_{12}$-like subtypes $P2Y_{12}$, $P2Y_{13}$, and $P2Y_{14}$ [1]. The numbers missing in this sequence correspond to non-mammalian orthologs or to receptors that have structural similarities but do not respond to nucleotides. The $P2Y_2$ receptor was first cloned in 1993 and initially named P_{2U} [2]. Its physiological agonists are adenosine-5′-triphosphate (ATP; **1a** in Fig. 1) and uridine-5′-triphosphate (UTP; **1b**) with similar potencies, as well as diadenosine tetraphosphate (Ap_4A; **1c**). $P2Y_2$ receptor activation leads to a stimulation of phospholipase C_β via $G\alpha_{q/11}$ protein coupling [3]. As a result, the second messengers inositol trisphosphate (IP_3) and diacylglycerol are produced that mediate the release of calcium ions from intracellular stores, and protein kinase C activation, respectively. In addition, the $P2Y_2$ receptor appears to couple to other G proteins as well, including G_o [4], G_{12} [5], and G_{16} [6].

$P2Y_2$ receptor mRNA is expressed in a range of different human organs and tissues, including skeletal muscle and heart, at more moderate levels in the spleen, intestine, immune cells, bone marrow, and lungs, as well as to a lower extent also in kidneys, liver, stomach, pancreas, bones, and different regions of the brain [7]. Functional $P2Y_2$ receptors were detected in epithelial and endothelial cells, smooth muscle cells, kidney tubules, cardiomyocytes, leukocytes, osteoblasts, as well as in cells of the central and peripheral nervous systems [1]. The $P2Y_2$ receptor is of pharmacological interest due to its significant potential as a drug target. $P2Y_2$ receptor knockout mice were found to exhibit defective chloride secretion in airway epithelium in response to ATP and UTP, which suggests that $P2Y_2$ receptor agonists could function as a treatment for patients suffering from cystic fibrosis by bypassing the defective chloride ion channel cystic fibrosis transmembrane conductance regulator (CFTR) [8]. $P2Y_2$ receptor agonism may possibly also find application in reducing post-ischemic myocardial damage, since cardioprotective effects were observed for the selective $P2Y_2$ receptor agonist uridine-5′-tetraphosphate δ-phenyl ester tetrasodium salt (MRS2768, compound **2** in Fig. 1) [9]. Furthermore, a neuroprotective role of the $P2Y_2$ receptor was postulated via the induction of α-secretase-dependent amyloid precursor protein processing in astrocytoma cells [10].

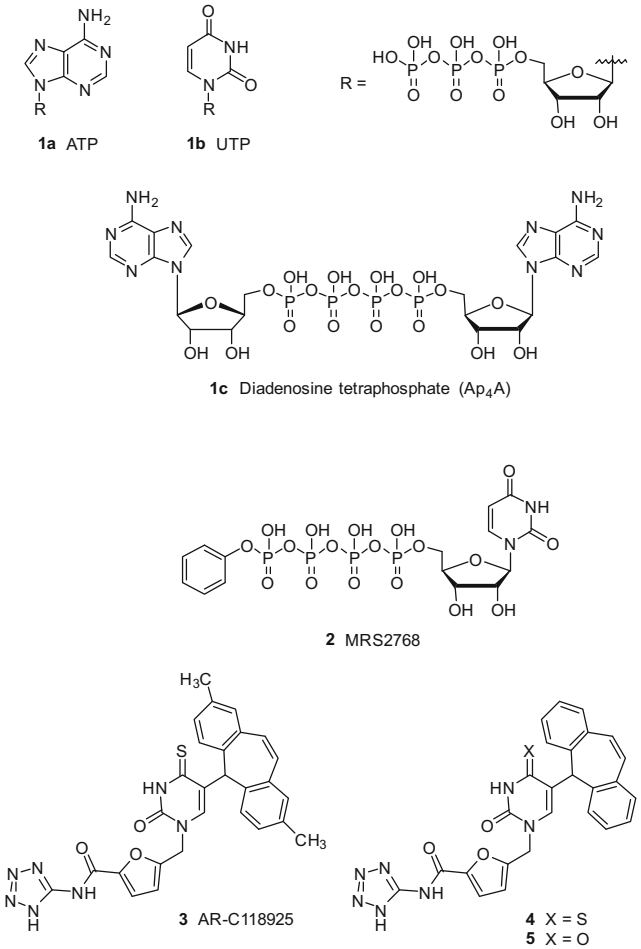

Fig. 1 Structures of the physiological $P2Y_2$ receptor agonists ATP (**1a**), UTP (**1b**), and diadenosine tetraphosphate (Ap_4A, **1c**), the selective $P2Y_2$ receptor agonist MRS2768 (**2**), the antagonist AR-C118925 (**3**), and its derivatives **4** and **5**

Blocking this receptor, on the other hand, could be useful for treating atherosclerosis and excessive inflammation, since the $P2Y_2$ receptor activates cytosolic phospholipase A_2, which in turn promotes the release of arachidonic acid and subsequent synthesis of prostaglandins and leukotrienes [11–15]. Furthermore, $P2Y_2$ receptor antagonists may be useful as novel cancer therapeutics, as the $P2Y_2$ receptor was shown to promote tumor metastasis via opening of the endothelial barrier [16]. Proliferation of different tumor and non-tumor cells [17–21], as well as the induction of cell cycle progression in vascular smooth muscle cells [22, 23], was also attributed to $P2Y_2$ receptor activation. Another potential benefit for $P2Y_2$ receptor antagonists could be for patients suffering from nephrogenic diabetes insipidus acquired, for example, through chronic use of lithium in a bipolar disorder therapy. The $P2Y_2$ receptor was found to be expressed in collecting ducts in the

kidney, where it opposes the actions of antidiuretic hormone (arginine vasopressin) and, thus, reduces water reuptake into the blood stream [24]. Additionally, the observation that $P2Y_2$ receptor activation inhibits bone formation by osteoblasts suggests that $P2Y_2$ receptor antagonism could further prove useful in the treatment of osteoporosis [25].

The fact that the $P2Y_2$ receptor is involved in signaling pathways that play a role in various pathological states highlights the strong need for potent and selective antagonists for this receptor. One of the most selective antagonists described to date is the thiouracil derivative 5-{[5-(2,8-dimethyl-5*H*-dibenzo[*a*,*d*]cycloheptен-5-yl)-3,4-dihydro-2-oxo-4-thioxo-1(2*H*)-pyrimidinyl]methyl}-*N*-(1*H*-tetrazol-5-yl)-2-furancarboxamide (AR-C118925, **3**, Fig. 1) [26, 27], which has been developed by structural modifications of the physiological agonist UTP [28]. Replacement of the ribose triphosphate moiety and derivatization of the uracil ring in UTP (**1b**) eliminated agonist properties and improved potency and pharmacokinetic properties, respectively [28]. AR-C118925 (**3**) is thought to be a useful pharmacological tool for in vitro as well as in vivo studies of $P2Y_2$ receptors [9, 29–31].

However, AR-C118925 (**3**) was until very recently not commercially available and, as a result, it has not been well characterized. Owing to the high demand for a selective $P2Y_2$ receptor antagonist, we re-synthesized AR-C118925 (**3**) together with two derivatives, established an optimized procedure, and assessed their antagonistic potential on the $P2Y_2$ receptor and related targets, including further subtypes of the P2Y receptor family, P2X receptor ion channels, adenosine receptors (P1 receptors), enzymes involved in nucleotide metabolism (ectonucleotidases), as well as a range of other potential targets that complement the selectivity testing previously published by Kemp et al. [27]. Comprehensive in vitro evaluation of AR-C118925 (**3**) provided in the present study, including physicochemical, pharmacokinetic, and pharmacological data will provide a basis for future in vivo studies.

Materials and methods

Materials and chemicals

All commercially available reagents and solvents for the syntheses were used without further purification. Petroleum ether with a boiling point of 40–60 °C was employed. Column chromatography was performed on silica gel 60. TLC plates coated with silica gel $60F_{254}$ were used. Melting points were determined on a Wepa "Apotec" melting point apparatus and are uncorrected. ^{1}H- and ^{13}C-NMR spectra were measured on a Bruker Avance 500 MHz spectrometer. The chemical shifts of the remaining protons of the deuterated solvent served as internal standard. Mass spectra were recorded on an MS-50 spectrometer at the Chemical Institute, University of Bonn (EI), and on an API 2000 (Applied Biosystems) at the Pharmaceutical Institute, University of Bonn (ESI, +*Q*: positive ion scan, −*Q*: negative ion scan).

Dulbecco's modified Eagle's medium (DMEM), trypsin-EDTA, fluo-4 acetoxymethyl ester (fluo-4 AM), lipofectamine 2000 and penicillin/streptomycin were purchased from Life Technologies GmbH (Darmstadt, Germany). Fetal bovine serum and Pluronic® F-127 were obtained from Sigma-Aldrich (Munich, Germany), G418 from Applichem (Darmstadt, Germany), Corning® 3340 microplates from Corning (Tewksbury, Massachusetts, USA) and Lumasafe liquid scintillation cocktail from Perkin-Elmer (Waltham, Massachusetts, USA). The Xfect™ Transfection Reagent kit was purchased from Clontech (Saint-Germain-en-Laye, France).

Syntheses

5-Bromouracil (11) [32] Uracil (**10**, 22.4 g, 0.20 mol) was suspended in water (200 ml). Bromine was added at room temperature (rt) until a yellow color remained (38 g, 0.24 mol). The clear, orange-colored solution was heated in an open vessel to remove solvent until a colorless solid precipitated. After cooling to rt, this solid was filtered off, washed with water (100 ml), and dried at 80 °C. 5-Bromouracil (36.8 g, 96.3 %) was obtained as a colorless solid. ^{1}H-NMR (500 MHz, DMSO) δ (ppm) = 7.87 (s, 1H), 11.19 (s, 1H, NH), 11.47 (s, 1H, NH). ^{13}C-NMR (500 MHz, DMSO) δ (ppm) = 94.6, 142.3, 151.0, and 160.2.

5-Bromo-2,4-dichloropyrimidine (12) [33, 34] A mixture of 5-bromouracil (**11**, 7.64 g, 40 mmol), *N*,*N*-dimethylaniline (7.3 g, 60 mmol) and freshly distilled phosphorus oxychloride (24 ml) was stirred at 120–130 °C for 80 min. After cooling to 50–60 °C, the resulting black solution was poured into ice-water. This mixture was extracted with dichloromethane (3 × 50 ml). The combined organic phases were washed with water (2 × 50 ml, for removal of dimethylanilinium chloride), aqueous sodium carbonate solution (1 × 50 ml), and brine (1 × 20 ml). After drying over magnesium sulfate, the organic phase was evaporated under reduced pressure. 5-Bromo-2,4-dichloropyrimidine (8.81 g, 96.6 %) was obtained as a dark red oil of low viscosity. ^{1}H-NMR (500 MHz, $CDCl_3$) δ (ppm) = 8.67 (s, 1H). ^{13}C-NMR (500 MHz,$CDCl_3$) δ (ppm) = 118.8, 158.9, 161.4, and 161.7.

5-Bromo-2,4-*bis*-(1,1-dimethylethoxy)pyrimidine (6) [35] A solution of bromo-2,4-dichloropyrimidine (**12**, 6.6 g, 29 mmol) in 20 ml anhydrous tetrahydrofuran (THF) was added to an ice-cooled suspension of potassium *tert*-butylate (13.5 g, 120 mmol) in 20 ml anhydrous THF over a period of 1 h. After stirring at rt for another 90 min, 40 ml of water was added. The mixture was extracted with ethyl acetate (3 × 20 ml). The combined organic phases were washed with

diluted aqueous HCl solution and subsequently with brine (10 ml each), dried over magnesium sulfate and evaporated under reduced pressure. The residual black oil was purified by column chromatography (40 g silica gel, toluene as eluent). 5-Bromo-2,4-*bis*-(1,1-dimethylethoxy)pyrimidine (4.67 g, 53 %) was obtained as a colorless oil which became a beige-colored solid upon storage at 4 °C. R_f = 0.3 (toluene). ^{1}H-NMR (500 MHz, $CDCl_3$) δ (ppm) = 1.58 (s, 9H), 1.63 (s, 9H), and 8.23 (s, 1H).

5-Methylfuran-2-carboxylic acid (14) [36] Upon cooling in an acetone/dry ice bath, a solution of 2-furancarboxylic acid (**13**, 2.24 g, 20 mmol, dried at 100 °C) in 20 ml anhydrous THF was added dropwise to a mixture of 33 ml (60 mmol) 1.8 M lithium diisopropylamide in THF/hexane/ethylbenzole (Aldrich) and 80 ml of anhydrous THF. After 15 min at −70 to −60 °C, a red-brown solution evolved, to which 2.5 ml (40 mmol) methyl iodide was added. The temperature was allowed to rise to 0 °C, and 80 ml of water was added. The mixture was washed with diethyl ether, and the organic phase was discarded. The aqueous phase was acidified with hydrochloric acid and extracted with diethyl ether (3 × 40 ml). The combined organic layers were washed with brine, dried over magnesium sulfate, filtered, and concentrated under reduced pressure. 5-Methylfuran-2-carboxylic acid (2.48 g, 92 %) was obtained as a beige-colored solid and used without further purification in the subsequent step. Purity, 93 %; main impurities, 2-furancarboxylic acid and ethylbenzene (NMR). ^{1}H-NMR (500 MHz, $CDCl_3$) δ (ppm) = 2.39 (s, 3H, CH_3), 6.15 (dd, J = 0.9 Hz, J = 3.4 Hz, 1H), 7.23 (d, J = 3.4 Hz, 1H), and 9.0–10.0 (s broad, 1H, COOH). ^{13}C-NMR (500 MHz, $CDCl_3$) δ (ppm) = 14.0, 109.0, 121.7, 147.3, 158.6, and 163.4. Quantification of main impurities: comparison of the integrations of the following signals: 2.71 (q, 2H) for ethylbenzene, 6.15 (dd, 1H) for the product, and 6.54 (dd, 1H) for 2-furancarboxylic acid.

5-Methylfuran-2-carboxylic acid ethyl ester (15) A solution of 5-methylfuran-2-carboxylic acid (2.52 g, 20 mmol) and dimethylformamide-diethylacetal (4.42 g, 40 mmol) in 30 ml anhydrous DMF was stirred at rt for 48 h. The resulting mixture was directly submitted to column chromatography using 80 g silica gel, and 5 % EtOH in CH_2Cl_2 as eluent. 5-Methylfuran-2-carboxylic acid ethyl ester (2.82 g, 92 %) was isolated as a yellowish oil. R_f = 0.6 (in pure CH_2Cl_2). Purity (NMR), 66 %; main impurities, 24 % furan-2-carboxylic acid ethyl ester and 10 % ethylbenzene (both imported from the previous step). ^{1}H-NMR (500 MHz, $CDCl_3$) δ (ppm) = 1.34 (t, J = 7.3 Hz, 3H), 2.36 (s, 3H, CH_3), 4.32 (q, J = 7.3 Hz, 2H), 6.09 (dq, J = 0.9 Hz, J = 3.5 Hz, 1H), and 7.05 (dd, J = 0.5 Hz, J = 3.5 Hz, 1H). ^{13}C-NMR (500 MHz, $CDCl_3$) δ (ppm) = 14.0, 14.4, 60.7, 108.3, 119.2, 143.3, 157.0, and 157.9.

5-(Bromomethyl)-furan-2-carboxylic acid ethyl ester (8) 5-Methylfuran-2-carboxylic acid ethyl ester (2.82 g, 12.8 mmol (considering the degree of purity)), *N*-bromosuccinimide (2.49 g, 14 mmol), and AIBN (0.1 g) were suspended in tetrachloromethane (30 ml) and stirred at 70 °C for 2 h. After cooling to rt, the solid was filtered off and washed with tetrachloromethane (5 ml). The combined filtrates were concentrated under reduced pressure. 5-(Bromomethyl)furan-2-carboxylic acid ethyl ester (3.69 g, 96 %) was obtained as a yellow oil and used without further purification. Purity (NMR), 68 mol% (78 mass%), a single impurity was present: 32 mol% (22 mass%) furan-2-carboxylic acid ethyl ester. ^{1}H-NMR (500 MHz, $CDCl_3$) δ (ppm) = 1.36 (t, J = 7.3 Hz, 3H), 4.35 (q, J = 7.3 Hz, 2H), 4.47 (s, 2H), 6.47 (d, J = 3.5 Hz, 1H), and 7.09 (d, J = 3.6 Hz, 1H).

5-(2,8-Dimethyl-5*H*-dibenzo[*a*,*d*]cyclohepten-5-yl)-2,4(1*H*,3*H*)-pyrimidinedione (16) 5-Bromo-2,4-*bis*-(1,1-dimethylethoxy)pyrimidine (**6**, 0.33 g, 1.1 mmol) was dissolved in anhydrous THF (10 ml). Upon cooling in an acetone/dry ice bath, a 2.5-M solution of *n*-butyl lithium in hexane (0.48 ml, 1.2 mmol) was added. After stirring for 20 min at that temperature, a solution of 2,8-dimethyl-5*H*-dibenzo[*a*,*d*]cyclohepten-5-one (**7**, 0.24 g, 1.0 mmol) in anhydrous THF (4 ml) was added. After stirring for another 2 h, the cooling bath was removed and the stirring was continued at rt for 4 h. After the addition of saturated aqueous ammonium chloride solution (10 ml), the mixture was extracted with ethyl acetate (3 × 20 ml). The combined organic layers were washed with brine, dried over magnesium sulfate, filtered, and concentrated under reduced pressure. Triethylsilane (1.0 ml, 6.3 mmol) and anhydrous CH_2Cl_2 were added to the residue. At 0 °C, trifluoroacetic acid (1.8 ml) was slowly added. The resulting blood-red solution was stirred at rt overnight, upon which it turned pale yellow. After the addition of toluene (4 ml), the mixture was concentrated under reduced pressure. This was repeated twice to remove all excess reagents. The residue was suspended in diethyl ether (40 ml), triturated with petroleum ether, and stored at 4 °C for 2 h. The solid was filtered off, washed with petroleum ether (10 ml), and dried at 60 °C. The colorless solid (244 mg) thus obtained was purified by column chromatography (40 g silica gel, first 500 ml of 2 % EtOH in CH_2Cl_2, then 4 % EtOH in CH_2Cl_2). 5-(2,8-Dimethyl-5*H*-dibenzo[*a*,*d*]cyclohepten-5-yl)-2,4(1*H*,3*H*)-pyrimidinedione (**16**, 190 mg, 58 %) was obtained as a colorless solid. R_f = 0.3 (CH_2Cl_2/EtOAc = 1:1). ^{1}H-NMR (500 MHz, DMSO) δ (ppm) = 2.27 (s, 6H, CH_3), 5.17 (s, 1H), 6.31 (s, 1H), 6.85 (s, 2H), 7.15 (m, 4H), 7.38 (d, J = 7.6 Hz, 2H), 10.33 (s, 1H, NH), and 10.84 (s, 1H, NH). ^{13}C-NMR (500 MHz, DMSO) δ (ppm) = 20.5, 48.7, 109.8, 129.6, 130.0, 130.8, 131.1, 134.3, 135.0, 135.8, 137.2, 151.0, and 163.3.

5-{[5-(2,8-Dimethyl-5*H*-dibenzo[*a,d*]cyclohepten-5-yl)-3,4-dihydro-2,4-dioxo-1(2*H*)pyrimidinyl]methyl}-2-furancarboxylic acid ethyl ester (17) 5-(2,8-Dimethyl-5*H*-dibenzo[*a,d*]cyclohepten-5-yl)-2,4(1*H*,3*H*)-pyrimidinedione (**16**, 0.19 mg, 0.59 mmol), hexamethyldisilazane (HMDS, 1 ml), and approximately 5 mg of finely ground ammonium sulfate were sealed in a pressure-resistant vial and heated to 140 °C (temperature of the oil bath) for 10 min. The resulting clear, orange-colored solution was cooled to rt 5-(bromomethyl)furan-2-carboxylic acid ethyl ester (**8**, 0.23 g, 1.0 mmol) and 5 mg of solid iodine were added, upon which a colorless solid precipitated. This mixture was heated to 140 °C for 60 min, upon which it turned brown. At rt, saturated aqueous sodium hydrogencarbonate solution (10 ml) was added. The mixture was extracted with ethyl acetate (3 × 10 ml). The combined organic layers were washed with brine, dried over magnesium sulfate, filtered, and concentrated under reduced pressure. The resulting brown compound was purified by column chromatography (40 g silica gel, starting with 400 ml of 2 % EtOH in CH_2Cl_2, then 4 % EtOH in CH_2Cl_2). 5-{[5-(2,8-Dimethyl-5*H*-dibenzo[*a,d*]-cyclohepten-5-yl)-3,4-dihydro-2,4-dioxo-1(2*H*)pyrimidinyl]methyl}-2-furancarboxylic acid ethyl ester (**17**, 182 mg, 64 %) was obtained as a crème-colored solid. R_f = 0.6 (CH_2Cl_2/EtOAc = 1:1). ^{1}H-NMR (500 MHz, $CDCl_3$) δ (ppm) = 1.43 (t, *J* = 7.3 Hz, 3H, $-CH_2-C\underline{H}_3$), 2.29 (s, 6H, 2 × CH_3), 4.42 (q, *J* = 7.3 Hz, 2H, $-C\underline{H}_2-CH_3$), 4.71 (s, 2H, $C-C\underline{H}_2-N$), 5.24 (s, 1H, dibenzosuberenone), 6.38 (d, *J* = 3.3 Hz, 1H, furane), 6.66 (d, *J* = 1.2 Hz, 1H, uracil), 6.75 (s, 2H, dibenzosuberenone), 7.07 (d, *J* = 1.1 Hz, 2H, dibenzosuberenone), 7.10 (d, *J* = 3.3 Hz, 1H, furane), 7.14 (dd, *J* = 1.3 Hz, *J* = 7.8 Hz, 2H, dibenzosuberenone), 7.35 (d, *J* = 7.8 Hz, 2H, dibenzosuberenone), and 8.33 (s, 1H, NH). ^{13}C-NMR (500 MHz, $CDCl_3$) δ (ppm) = 14.4, 20.9, 43.9, 49.5, 61.2, 111.9, 112.0, 118.6, 129.9, 130.4, 131.0, 134.2, 134.3, 136.6, 140.0, 145.2, 150.1, 152.3, 158.4, and 162.4.

5-{[5-(2,8-Dimethyl-5*H*-dibenzo[*a,d*]cyclohepten-5-yl)-3,4-dihydro-2-oxo-4-thioxo-1(2*H*)-pyrimidinyl]methyl}-2-furancarboxylic acid (19) 5-{[5-(2,8-Dimethyl-5*H*-dibenzo[*a,d*]cyclohepten-5-yl)-3,4-dihydro-2,4-dioxo-1(2*H*)pyrimidinyl]methyl}-2-furancarboxylic acid ethyl ester (**17**, 225 mg, 0.45 mmol), Lawesson's reagent (0.28 g, 0.7 mmol) and anhydrous dioxane (4 ml) were sealed in a pressure-resistant vial and heated to 120 °C (temperature of the oil bath) for 3 h. After cooling to rt, water (1 ml), methanol (2 ml) and lithium hydroxide (until alkaline reaction) were added. After stirring at rt for 1 h, water (10 ml) and hydrochloric acid (until acidic reaction could be observed) were added. After cooling to 4 °C, the brown precipitate was filtered off, washed with water, dried in a desiccator, and purified by column chromatography (40 g silica gel, 5 % acetic acid in CH_2Cl_2). 5-{[5-(2,8-Dimethyl-5*H*-dibenzo[*a,d*]cyclohepten-5-yl)-3,4-dihydro-2-oxo-4-thioxo-1(2*H*)-pyrimidinyl]methyl}-2-furancarboxylic acid (**15**, 123 mg, 58 %) was thus obtained as a yellow solid. R_f = 0.5 (5 % acetic acid in CH_2Cl_2). ^{1}H-NMR (500 MHz, DMSO) δ (ppm) = 2.26 (s, 6H, 2 x CH_3), 4.90 (s, 2H, $C-C\underline{H}_2-N$), 5.72 (s, 1H, dibenzosuberenone), 6.58 (d, *J* = 3.5 Hz, 1H, furane), 6.73 (s, 2H, dibenzosuberenone),6.92 (s, 1H, uracil), 7.09 (s, 2H, dibenzosuberenone), 7.12 (d, *J* = 7.4 Hz, 2H, dibenzosuberenone), 7.23 (d, *J* = 3.5 Hz, 1H, furane), 7.42 (d, *J* = 7.9 Hz, 2H, dibenzosuberenone), and 12.59 (s, 1H, NH).

5-{[5-(2,8-Dimethyl-5*H*-dibenzo[*a,d*]cyclohepten-5-yl)-3,4-dihydro-2-oxo-4-thioxo-1(2*H*)-pyrimidinyl]methyl}-*N*-(1*H*-tetrazol-5-yl)-2-furancarboxamide (AR-C118925, 3) A mixture of 5-{[5-(2,8-dimethyl-5*H*-dibenzo[*a,d*]-cyclohepten-5-yl)-3,4-dihydro-2-oxo-4-thioxo-1(2*H*)-pyrimidinyl]methyl}-2-furancarboxylic acid (**19**, 47 mg, 0.1 mmol), aminotetrazole hydrate (21 mg, 0.2 mmol), 8-hydroxybenzotriazole (27 mg, 0.2 mmol), diisopropylcarbodiimide (25 mg, 0.2 mmol), and anhydrous tetrahydrofuran (THF, 0.5 ml) was stirred at rt for 6 h. After the addition of water (5 ml) and alkalization with aqueous ammonia solution, the mixture was filtered through a 0.47-µm filter. The filtrate was acidified by the addition of hydrochloric acid and left to stand at 4 °C for several hours. The newly formed precipitate was filtered off and washed with cold water (2 × 2 ml). 5-{[5-(2,8-Dimethyl-5*H*-dibenzo[*a,d*]cyclohepten-5-yl)-3,4-dihydro-2-oxo-4-thioxo-1(2*H*)-pyrimidinyl]methyl}-*N*-(1*H*-tetrazol-5-yl)-2-furancarboxamide (**3**, 45 mg, 75 %) was obtained as a yellow solid.

Retroviral transfection of 1321N1 astrocytoma cells with human $P2Y_1$, $P2Y_4$, $P2Y_6$, and $P2Y_{11}$, rat $P2Y_6$, and P2X receptor subtypes

Transfection was performed as previously described [37]. Briefly, the coding sequence of the respective receptor was cloned into the pQCXIN or pLXSN retroviral vector, amplified, purified, and sequenced prior to the transfection of GP^+envAM-12 packaging cells together with vesicular stomatitis virus G (VSV-G) protein DNA using lipofectamine 2000. After 16 h, 3 ml of DMEM containing 10 % fetal bovine serum, 1 % of a penicillin/streptomycin solution (final concentrations: penicillin = 100 U/ml, streptomycin = 0.1 mg/ml), and sodium butyrate (5 mM) was given to the packaging cells, and these were kept at 32 °C and 5 % CO_2 for 48 h, during which the viral vectors containing the receptor sequence were produced and released into the surrounding medium. These were harvested, filtered (45 µm filter pore diameter) and given to 1321N1 astrocytoma cells that do not intrinsically express P2 receptors at a detectable level. Polybrene solution (6 µl, 4 mg/ml in H_2O, filtered) was added. After 2.5 h, the virus-

containing medium was discarded and DMEM supplemented with 10 % fetal bovine serum and 1 % of a penicillin/streptomycin solution (final concentrations: penicillin = 100 U/ml, streptomycin = 0.1 mg/ml) was given to the cells. These were incubated for 2 days, followed by selection of successfully transfected cells with geneticin resistance by adding G418 (200 μg/ml) to the medium. Single cells were selected and grown into monoclonal colonies for the $P2Y_4$ receptor and the P2X receptor cell lines; polyclonal cell lines were used in case of the human $P2Y_{1,6,11}$ and the rat $P2Y_6$ receptors.

Lentiviral transfection of 1321N1 astrocytoma cells with the human and rat $P2Y_2$ receptors

The coding sequence of the $P2Y_2$ receptor was cloned into the pLVX-IRES-mCherry vector, amplified, purified and sequenced prior to transfection of HEK-293T packaging cells using the Xfect™ Transfection Reagent kit. DMEM containing 10 % fetal bovine serum and 1 % of a penicillin/streptomycin solution (final concentrations: penicillin = 100 U/ml, streptomycin = 0.1 mg/ml) was given to the packaging cells and these were kept at 37 °C and 5 % CO_2 for 4 h, with sodium butyrate (5 mM) added to the nutrient medium. The packaging cells were incubated at 32 °C and 5 % CO_2 for 48 h, during which the viral vectors containing the $P2Y_2$-IRES-mCherry sequence were produced and released into the surrounding medium. These were harvested, filtered (45 μm filter pore diameter), and given to 1321 N1 astrocytoma cells that do not intrinsically express P2Y receptors at a detectable level. Polybrene solution (6 μl, 4 mg/ml in H_2O, sterile filtered) was added. After 2.5 h, the virus-containing medium was discarded and DMEM supplemented with 10 % fetal bovine serum and 1 % of a penicillin/streptomycin solution (final concentrations: penicillin = 100 U/ml, streptomycin = 0.1 mg/ml) was given to the cells. Using fluorescence-activated cell sorting, individual cells were selected that emitted a high intensity of fluorescent light by the mCherry protein at 610 nm following excitation at a wavelength of 587 nm, and subsequently grown into monoclonal colonies. A high intensity of fluorescent light corresponds to a high expression of mCherry, which in turn is directly proportional to $P2Y_2$ receptor expression, since the coding sequences for both proteins were transfected together but separated by an internal ribosome entry site (IRES).

Cell culturing

1321N1 human astrocytoma cells stably transfected with the coding sequence for the respective receptor were grown in DMEM supplemented with 10 % fetal bovine serum, 1 % of a penicillin/streptomycin solution (final concentrations: penicillin = 100 U/ml, streptomycin = 0.1 mg/ml), and, for cell lines that carry geneticin resistance, 200 μg/ml G418. Chinese hamster ovary (CHO) cells were grown in DMEM/F12 with the supplements above, in addition to hygromycin (300 μg/ml). The cells were kept at 37 °C in humidified air containing 5 % carbon dioxide. The cells were maintained in the exponential growth phase throughout and regularly tested for mycoplasma contamination.

Calcium mobilization assays for $P2Y_1$, $P2Y_2$, $P2Y_4$, and $P2Y_6$ receptors

Calcium measurements were performed as previously described [38]. Briefly, 1321N1 human astrocytoma cells stably transfected with the coding sequence for the respective P2Y receptor were used. Approximately 24 h prior to testing, the nutrient medium was discarded and the cells rinsed with phosphate-buffered saline before detachment using 0.05 % trypsin/0.6 mM EDTA. The cells were then suspended in DMEM with the supplements described above and dispensed into sterile, black, flat, clear bottom 96-well polystyrene microplates with lid (Corning® 3340) at 50,000 cells per well. The microplates were incubated at 37 °C in humidified air with 5 % carbon dioxide, during which the cells adhered to the coated bottom of the wells. Test compounds were investigated by measuring their inhibition of $P2Y_1$, $P2Y_2$, $P2Y_4$, or $P2Y_6$ receptor-mediated intracellular calcium mobilization using a FlexStation 3 (Molecular Devices GmbH, Biberach an der Riss, Germany) plate reader. At the start of the assay, the plated cells were loaded with fluo-4 AM (Life Technologies GmbH, Darmstadt, Germany) for 1 h. Excess dye was subsequently removed and HBSS buffer given to the cells. Afterwards, the cells were pre-incubated with the test compound for 30 min. Using the pipetting function of the microplate reader, the physiological ligand was injected at a concentration that corresponds to its EC_{80}: 500 nM ADP for the $P2Y_1$, 500 nM UTP for the $P2Y_2$ and $P2Y_4$, and 750 nM UDP for the $P2Y_6$ receptor. The final volume was 200 μl/well. Fluorescence was measured at 525 nm following excitation at 488 nm. At least three independent experiments were performed in duplicates. IC_{50} values for antagonists were calculated by non-linear regression using Prism® 5.0 (GraphPad Software, San Diego, CA, USA).

Calcium mobilization assays for $P2Y_{11}$ and P2X receptors

The calcium measurements for the $P2Y_{11}$ and P2X receptors have also been described before [37]. In summary, 1321N1 human astrocytoma cells stably transfected with the coding sequence for the respective receptor were harvested with 0.05 % trypsin/0.6 mM EDTA and rinsed with culture medium. The cells were kept at 37 °C in humidified air containing 5 % carbon dioxide for 45 min and then centrifuged for 5 min at 200×*g* and 4 °C. After that, the cells were incubated for 1 h at 25 °C in Krebs-Ringer-HEPES buffer, pH 7.4, containing 3 μM Oregon

Green BAPTA-1/AM and 1 % Pluronic® F127. The cells were washed three times with Krebs-Ringer-HEPES buffer, diluted, and plated into black 96-well plates with clear bottoms at a density of approximately 16,000 cells/well and left to settle for 20 min. Fluorescence intensity was measured at 520 nm for 30 s at 0.4 s intervals using a Novostar® microplate reader (BMG Labtechnologies, Offenburg, Germany). The excitation wavelength was 485 nm. The respective agonist at a concentration that corresponds to its EC_{80} in buffer was injected using the automatic pipetting function of the microplate reader. At least three independent experiments were performed in duplicates, and IC_{50} values for antagonists were calculated by non-linear regression using Prism® 5.0 (GraphPad Software, San Diego, CA, USA).

Expression of the human $P2Y_2$, $P2Y_{12}$, and $P2Y_{14}$ receptors in CHO cells for β-arrestin translocation assays

CHO cells expressing β-arrestin fused to an N-terminal deletion mutant of β-galactosidase were stably transfected with the respective human receptor and cloned into the pCMV-ProLink-1 ($P2Y_2$ and $P2Y_{12}$) or pCMV-ProLink-2 ($P2Y_{14}$) vector tagged with a complementary enzyme fragment. The pCMV-ProLink-1 and pCMV-ProLink-2 vectors as well as the CHO cell line were purchased from DiscoverX (Fremont, CA, USA). Successfully transfected cells were selected using G418 (800 μg/ml) and cultured in F12 medium containing 10 % fetal calf serum, 100 units/ml penicillin G, 100 μg/ml streptomycin, 300 μg/ml hygromycin B, and 200 μg/ml G418 (Invitrogen, Carlsbad, CA, USA). Single cells were selected and grown into monoclonal colonies for the $P2Y_{14}$ receptor cell line; polyclonal cell lines were used for the $P2Y_2$ and $P2Y_{12}$ receptors. Upon activation of the receptor, β-arrestin tagged with the β-galacatosidase fragment is recruited to the receptor and the two enzyme fragments are combined to form a functional β-galactosidase enzyme. This interaction can be detected using a chemiluminescent substrate.

β-Arrestin translocation assays

The β-arrestin assays were performed as previously described for other GPCRs [39]. One day prior to the start of the assay, cells were detached from the culture flask using cell dissociation buffer (2 mM EDTA, 10 mM glucose in phosphate-buffered saline) and seeded into 96-well plates (ThermoScientific, Waltham, MA, USA) at a density of 25,000 cells per well in 90 μl Opti-MEM® medium supplemented with 2 % fetal calf serum, 100 units/ml penicillin G, 100 μg/ml streptomycin, 300 μg/ml hygromycin B, and 200 μg/ml G418 (Invitrogen, Carlsbad, CA, USA). Test compounds were diluted in DMSO and further diluted a tenfold in the medium described above. The final concentration of DMSO was 0.5 % in each case. Subsequently, 5 μl of this compound solution was given to each well and, after 30 min of incubation, 5 μl of agonist dissolved in cell seeding medium was added. For $P2Y_2$ receptor antagonist curves, the endogenous ligand UTP was used at a final concentration of 3 μM, which corresponds to the EC_{80} value. After 90 min of incubation, 50 μl of detection reagent (DiscoverX, Fremont, CA, USA) were given to each well. Luminescence was determined after a further 60 min using a Topcount NXT plate reader (Perkin-Elmer, Meriden, CT, USA). The data was analyzed using Prism® 5.0 (GraphPad Software, San Diego, CA, USA).

Results and discussion

Synthesis

The synthesis of AR-C118925 (**3**) had previously only been described in the patent literature [35]. We decided to follow the described general synthetic route (Scheme 1) but modified and optimized the individual reaction steps.

As depicted in Scheme 1, the target compound **3** is built from four precursors: the activated and protected uracil derivative **6**, which is fused to 2,8-dimethyldibenzosuberenone (**7**) and subsequently deprotected. Next, the product is coupled to the methylfurancarboxylic acid derivative **8**. After thioation and subsequent deprotection, the resulting free acid is coupled to aminotetrazole (**9**).

5-Bromo-2,4-*bis*-(1,1-dimethylethoxy)pyrimidine (**6**) was synthesized according to the described procedure [35] by bromination of uracil (**10**) in the 5-position with bromine resulting in 5-bromouracil (**11**). Subsequent chlorination of the keto-groups by treatment of **11** with phosphorus oxychloride yielded **12** [32]. It was found that addition of the base *N*,*N*-dimethylaniline in the chlorination step greatly sped up the reaction, also leading to increased yields. Reaction with potassium *tert*-butylate led to the desired building block **6** (Scheme 2).

The synthesis of 2,8-dimethyldibenzosuberenone (building block **7**, Scheme 1) was achieved as previously described [40], by modifying procedures laid down in a patent by Wild et al. [41].

5-(Bromomethyl)furan-2-carboxylic acid ethyl ester (**8**) was synthesized from 2-furancarboxylic acid in three steps (Scheme 3). The first step, leading to 5-methylfuran-2-carboxylic acid (**14**), a selective lithiation/methylation procedure, was inspired by the work of Knight and Nott [36]. It proved to be crucial that a large volume of solvent was used, as otherwise salts precipitated and a mixture of products was formed. The introduction of the ethyl ester could be easily achieved with dimethylformamide-diethylacetal. Stirring of 5-methylfuran-2-carboxylic acid (**14**) with that reagent in DMF

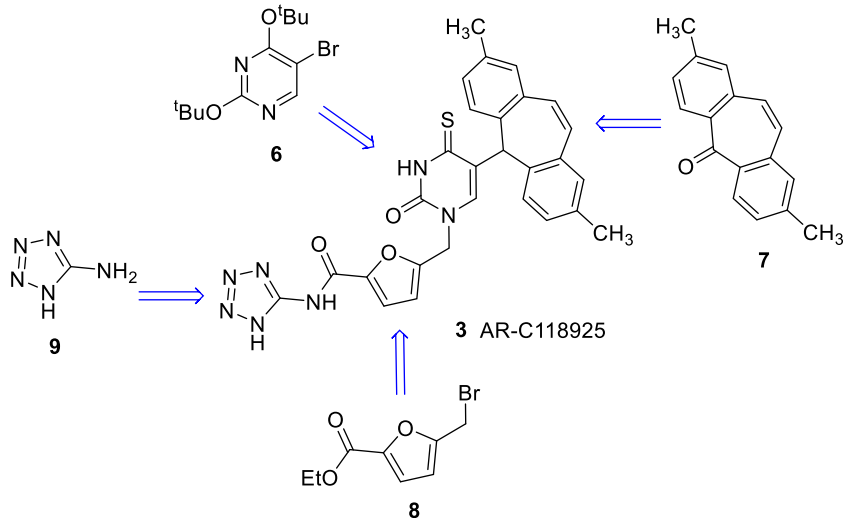

Scheme 1 Retrosynthetic analysis for the general synthetic strategy to obtain AR-C118925 (**3**)

at room temperature for 2 days led to 5-methylfuran-2-carboxylic acid ethyl ester (**15**) in yields of up to 91 %. The bromination of **15** afforded 5-(bromomethyl)furan-2-carboxylic acid ethyl ester (**8**) in high yield. The fact that building block **8** produced on a gram-scale contained furan-2-carboxylic acid ethyl ester as an impurity proved to be negligible as it did not take part in the next reaction step. Also, it can easily be separated from 5-{[5-(2,8-dimethyl-5*H*-dibenzo[*a,d*]cyclohepten-5-yl)-3,4-dihydro-2,4-dioxo-1(2*H*)-pyrimidinyl]methyl}-2-furancarboxylic acid ethyl ester (**17**, Scheme 4) upon purification by column chromatography.

5-Bromo-2,4-*bis*-(1,1-dimethylethoxy)pyrimidine (**6**) and 2,8-dimethyldibenzosuberenone (**7**) were coupled in a three-step reaction sequence. After lithiation, 5-bromo-2,4-*bis*-(1,1-dimethylethoxy)pyrimidine (**6**) was reacted with 2,8-dimethyldibenzosuberenone (**7**). The resulting alcohol was not purified but directly reduced to 5-(2,8-dimethyl-5*H*-dibenzo[*a,d*]cyclohepten-5-yl)-2,4(1*H*,3*H*)-pyrimidinedione (**16**) with triethylsilane/trifluoroacetic acid. As 2,8-dimethyldibenzosuberenone (**7**) is difficult to synthesize, a slight excess of 5-bromo-2,4-*bis*-(1,1-dimethylethoxy)pyrimidine (**6**) was used, leading to a yield of 50–60 %. If the commercially available unsubstituted dibenzosuberenone was employed in a twofold excess, a yield of up to 74 % of product (unmethylated **16**) was obtained.

In the next step, 5-(bromomethyl)furan-2-carboxylic acid ethyl ester (**8**) was coupled with 5-(2,8-dimethyl-5*H*-dibenzo[*a,d*]cyclohepten-5-yl)-2,4(1*H*,3*H*)-pyrimidinedione (**16**) using hexamethyldisilazane (HMDS) to give 5-{[5-(2,8-dimethyl-5*H*-dibenzo[a,d]cyclohepten-5-yl)-3,4-dihydro-2,4-dioxo-1(2*H*)-pyrimidinyl]methyl}-2-furancarboxylic acid ethyl ester (**17**). Product **17** was then thioated and deethylated in a one-pot procedure: After thioation, 5-{[5-(2,8-dimethyl-5*H*-dibenzo[a,d]cyclohepten-5-yl)-3,4-dihydro-2-oxo-4-thioxo-1(2*H*)-pyrimidinyl]methyl}-2-furancarboxylic acid ethyl ester (**18**) was hydrolyzed in situ to provide 5-{[5-(2,8-dimethyl-5*H*-dibenzo[*a,d*]cyclohepten-5-yl)-3,4-dihydro-2-oxo-4-thioxo-1(2*H*)-pyrimidinyl]methyl}-2-furancarboxylic acid (**19**) in 58 % yield.

The synthesis of the final product (**3**) was achieved by using a mixture of diisopropylcarbodiimide and 8-hydroxybenzotriazole (HOBt). AR-C118925 (**3**) could thus be isolated by a separation based on the acidity of the compound in a yield of 75 %.

The analogs **4** and **5** were obtained by the same procedure as AR-C118925 (**3**) using the commercially available dibenzosuberenone, a derivative of building block **7** lacking the two methyl groups.

The synthesis of the $P2Y_2$ receptor antagonist AR-C118925 (**3**) has two bottlenecks: (i) the difficult accessibility of 2,8-dimethyldibenzosuberenone (**7**) [40] and (ii) the moderate yields of the steps leading to compounds **16**, **17**, and **19** (50, 64, and 58 %, respectively). The total yield of the synthesis was as follows, depending on the starting materials considered: the whole synthesis from uracil (**10**) to **3** gave an overall yield of approximately 7 %. This is acceptable, as the reaction sequence from uracil to 5-bromo-2,4-*bis*-(1,1-dimethylethoxy)pyrimidine (**6**) can be easily performed on a multi-gram scale. Starting the

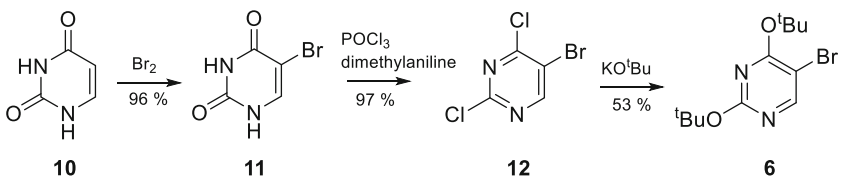

Scheme 2 Synthesis of building block **6**

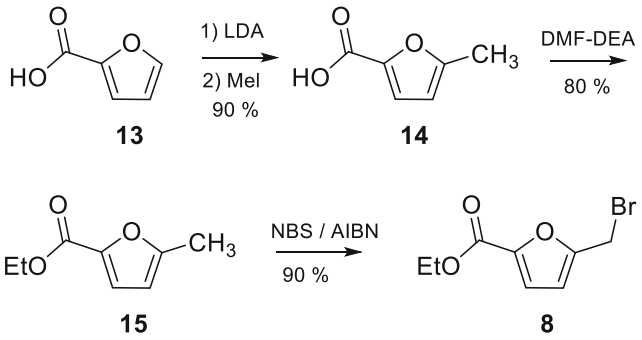

Scheme 3 Synthesis of building block **8** (*LDA* lithium diisopropylamide, *DMF-DEA* dimethylformamide-diethylacetal, *NBS* *N*-bromosuccinimide, *AIBN* azobisisobutyronitrile)

calculation from 2,8-dimethyldibenzosuberenone (**7**), the overall yield was approximately 16 %. If 2-furancarboxylic acid (**13**) is taken as a starting point, an overall yield of approximately 10 % could be achieved. In that case, the low efficiency of the coupling of 5-(bromomethyl)furan-2-carboxylic acid ethyl ester (**8**) to 5-(2,8-dimethyl-5*H*-dibenzo[*a*,*d*]cyclohepten-5-yl)-2,4(1*H*,3*H*)-pyrimidinedione (**16**) significantly impairs higher yields.

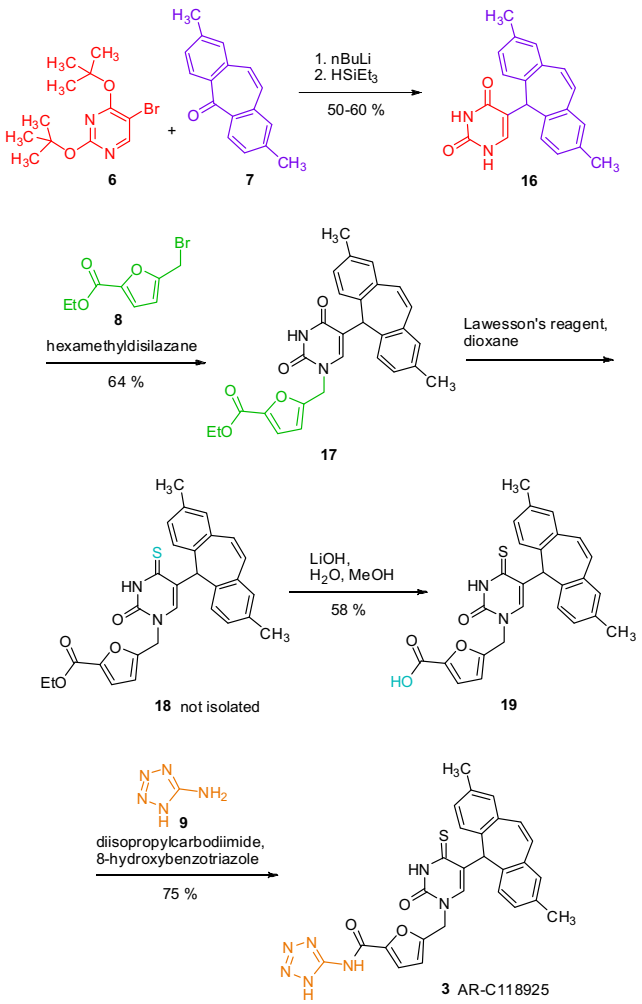

Scheme 4 Synthesis of AR-C118925 (**3**) by assembly of the building blocks

Pharmacological evaluation of AR-C118925 (3) and its derivatives on the P2Y$_2$ receptor and related targets

Despite its great potential as a pharmacological tool, the P2Y$_2$ receptor antagonist AR-C118925 (**3**) has not been extensively characterized so far. Kemp et al. [27] found it to be inactive at a concentration of 10 μM on a number of different receptors. These included the following human GPCRs: the serotonin receptors 5-HT$_{1A}$, 5-HT$_{2A}$, 5-HT$_{2B}$, 5-HT$_{2C}$, 5-HT$_6$, and 5-HT$_7$, the adrenergic receptors α_1, α_{2A}, α_{2B}, α_{2C}, β_1, and β_2, the cannabinoid receptor CB$_1$, the dopamine receptors D$_1$, D$_2$Lh, D$_3$, and D$_4$, the muscarinic acetylcholine receptors M$_1$, M$_2$, M$_3$, M$_4$, and M$_5$, the histamine receptors H$_1$ and H$_2$, the tachykinin receptors NK$_1$ and NK$_2$, the opioid receptors δ, κ, and μ, GABA$_B$, as well as the rat P2Y$_1$ receptor. The panel further included the following human ion channels: 5-HT$_3$, L-type and N-type calcium and ATP-sensitive potassium channels. They further assessed the human P2Y$_2$ receptor for antagonism in a sandwich enzyme-linked lectin assay measuring mucin secretion, where they determined an IC$_{50}$ value of approximately 1 μM upon receptor stimulation with 100 μM ATPγS [27].

In the present study, we have tested AR-C118925 (**3**) further and evaluated it together with two derivatives on other receptors and enzymes that are related to the P2Y$_2$ receptor. We found, as expected, that AR-C118925 (**3**) and its derivative **5** did not activate the human P2Y$_2$ receptor itself at a high concentration of 100 μM (data not shown). We subsequently assessed AR-C118925 (**3**) and its derivatives **4** and **5** for antagonism on a range of different targets. In all antagonist assays, the respective agonists for receptor stimulation were used at concentrations that correspond to their EC$_{80}$ values.

Out of all of the targets that we have tested, AR-C118925 (**3**) had the greatest antagonistic effect on the human P2Y$_2$ receptor, as expected, with an IC$_{50}$ value of 0.0721 ± 0.0124 μM when stimulating with 500 nM UTP (**1b**), and an virtually identical value of 0.0574 ± 0.0196 μM vs. 500 nM ATP (**1a**) (Fig. 2a). On the rat ortholog of the P2Y$_2$ receptor, AR-C118925 (**3**) displayed an IC$_{50}$ of 0.291 ± 0.047 μM (Fig. 2b) vs. 500 nM UTP, which was in the same range as that found on the human P2Y$_2$ receptor (4-fold lower). These results were obtained using the calcium mobilization assay. In an alternative in vitro system, the β-arrestin assay, the potency for AR-C118925 (**3**) vs. UTP was approximately a 10-fold lower (IC$_{50}$ = 0.716 ± 0.044 μM, Fig. 3a). When using diadenosine tetraphosphate (AP$_4$A) as the agonist, the potency was similar (4-fold lower; IC$_{50}$ = 0.191 ± 0.024 μM, Fig. 3b).

At the human P2Y$_4$ receptor, AR-C118925 (**3**) inhibited UTP-induced receptor activation with an IC$_{50}$ value of

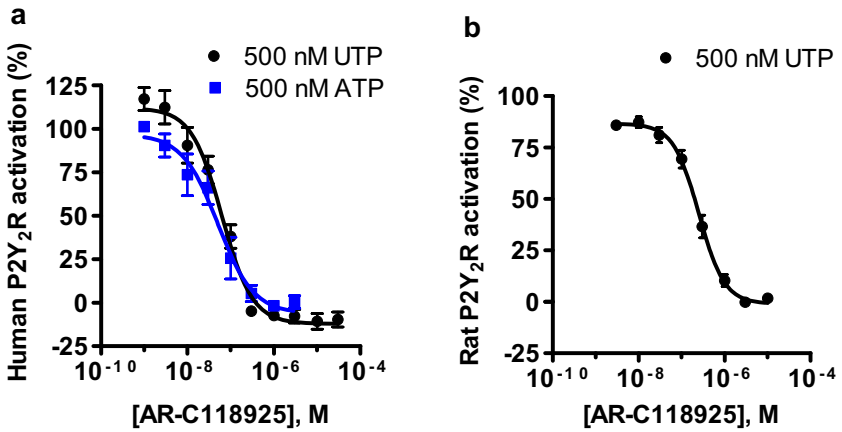

Fig. 2 Dose-response curves of AR-C118925 (**3**) on the **a** human and **b** rat $P2Y_2$ receptors in recombinant 1321N1 astrocytoma cells determined using the calcium mobilization assay with UTP (*black circles*) or ATP (*blue squares*) as agonists. The concentrations of the agonists used correspond to their EC_{80} values. For the human $P2Y_2$ receptor (**a**), IC_{50} values of 0.0721 ± 0.0124 μM vs. 500 nM UTP and 0.0574 ± 0.0196 μM vs. 500 nM ATP were determined. For the rat $P2Y_2$ receptor (**b**), an IC_{50} value of 0.291 ± 0.047 μM was obtained vs. 500 nM UTP. Data points are means of 6–8 independent experiments performed in duplicates ± standard error of the mean (SEM)

37.1 ± 7.2 μM. The $P2Y_4$ receptor is both structurally and pharmacologically most closely $P2Y_2$ receptor-related. The fact that AR-C118925 (**3**) is at least 500-fold selective for the $P2Y_2$ over the $P2Y_4$ receptor makes this compound a valuable tool compound, especially for studies in cells and tissues where these two receptors are simultaneously expressed [7].

The IC_{50} value of AR-C118925 (**3**) on the human $P2Y_1$ receptor was determined, using the calcium mobilization assay, to be 36.9 ± 2.7 μM, while on the human $P2Y_6$ receptor it was 30.4 ± 3.1 μM, meaning that the compound is also only weakly potent on the $P2Y_1$ and $P2Y_6$ receptors, and more than 400-fold selective for the $P2Y_2$ receptor over these other P2Y receptor subtypes. On the rat $P2Y_6$ receptor, on the other hand, AR-C118925 (**3**) appeared inactive. However, AR-C118925 (**3**) was more potent on the human $P2Y_{11}$ receptor, where we determined an IC_{50} value of 4.02 ± 0.73 μM. This is rather unexpected, since the sequence homology is greater between the $P2Y_2$ receptor and the $P2Y_1$ and $P2Y_6$ subtypes than between the $P2Y_2$ and $P2Y_{11}$ receptors. Yet, it is still over 50-fold selective for $P2Y_2$ over this receptor.

Using the β-arrestin assay, AR-C118925 (**3**) has also been assessed on the $P2Y_{12}$ and $P2Y_{14}$ receptors, where it showed low potency (IC_{50} of 33.7 ± 2.7 μM on $P2Y_{12}$ and 26 % inhibition of $P2Y_{14}$ at 3 μM). We, therefore, determined that AR-C118925 (**3**) is at least 50-fold selective for the $P2Y_2$ receptor over any other mammalian P2Y receptor subtype (Fig. 4; Table 1) with the exception of the $P2Y_{13}$ receptor, at which we could not do any assessments.

Derivative **4**, which lacks the two methyl groups on the tricyclic moiety, was found to be similarly potent on the human $P2Y_2$ and $P2Y_4$ receptors with IC_{50} values of 5.45 ± 1.07 and 9.42 ± 4.84 μM, respectively. Thus, the methyl groups on the tricyclic moiety appear to be important for affinity to the $P2Y_2$ receptor as well as for selectivity for the $P2Y_2$ over the $P2Y_4$ receptor. Derivative **4** was more active on the $P2Y_4$ receptor than AR-C118925 (Table 1). On the rat ortholog of the $P2Y_6$ receptor, it was only very weakly potent (Table 1).

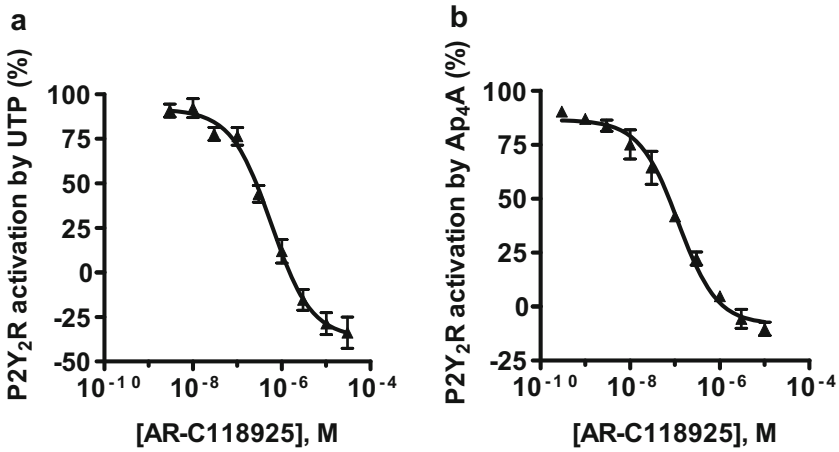

Fig. 3 Dose-response curves of AR-C118925 (**3**) on the human $P2Y_2$ receptor in recombinant CHO cells determined using the β-arrestin assay with **a** 3 μM UTP and **b** 4 μM diadenosine tetraphosphate (AP_4A) as agonists. The concentrations of the agonists correspond to their EC_{80} values; IC_{50} = 0.716 ± 0.044 μM vs. UTP and 0.191 ± 0.024 μM vs. AP_4A. Data points are the means of three to five independent experiments performed in duplicates ± SEM

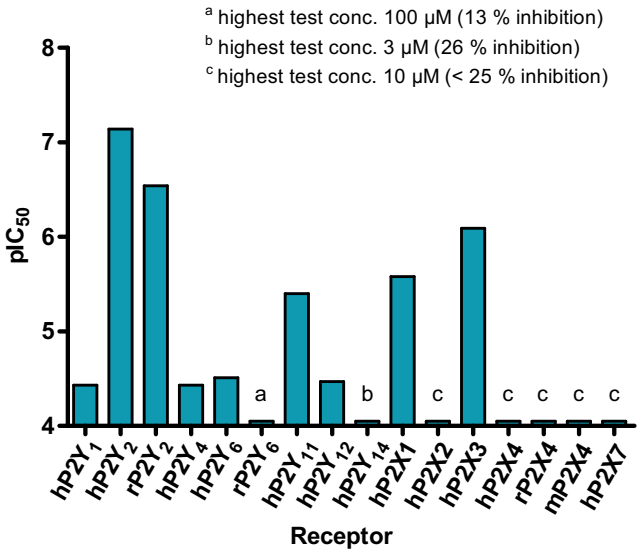

Fig. 4 Potency of AR-C118925 (**3**) on different P2 receptors, determined using the calcium mobilization assay, except for $P2Y_{12}$ and $_{14}$, which were assessed using the β-arrestin assay. *h* human, *r* rat, *m* mouse

The derivative **5**, which is an oxo-analog of **4**, was significantly less potent than AR-C118925 (**3**) or completely inactive on any of the tested P2Y receptor subtypes (Table 1). On the human $P2Y_2$ receptor, it shows only 49 % inhibition at 100 μM in the calcium mobilization assay and an IC_{50} value of 149 ± 14 μM in the β-arrestin assay. The thiouracil is, thus, vital for activity.

We additionally assessed AR-C118925 (**3**) and its derivative **5** on P2X receptor ion channels. Owing to the limited availability, derivative **4** could not be evaluated at targets other than selected P2Y receptors. While no significant effect was seen for AR-C118925 on the human P2X2, human, mouse and rat P2X4, and human P2X7 receptors (Table 2), notable antagonism was observed at the human P2X1 (IC_{50} = 2.63 ± 0.49 μM) and the human P2X3 receptors (IC_{50} = 0.819 ± 0.102 μM). AR-C118925 is, thus, still almost 50-fold selective for the $P2Y_2$ vs. the P2X1 receptor, but only 14-fold selective over the P2X3 receptor. Out of all the targets we tested, AR-C118925 is, besides the $P2Y_2$ receptor, most potent at the P2X3 ion channel. This should be considered when performing biological studies. Compound **5** also antagonized the human P2X3 receptor (IC_{50} = 7.45 ± 0.52 μM), and is, in fact, over 10-fold more potent at the P2X3 than at the $P2Y_2$ receptor. On the other P2X receptors, compound **5** had little effect (Table 2).

We evaluated AR-C118925 (**3**) and derivative **5** not only on P2 receptors, but also on all human adenosine receptor subtypes using radioligand receptor binding assays. On the adenosine A_{2A} receptor, AR-C118925 (**3**) displayed a K_i of 9.16 ± 1.57 μM but little effect was observed on the other three adenosine receptor subtypes (Table 3). Derivative **5**, on the other hand, antagonized the adenosine A_3 receptor (K_i = 11.2 ± 2.3 μM) but not the other subtypes (Table 3).

On the human nucleotide pyrophosphatase 1 (NPP1), AR-C118925 (**3**) acted as a weak inhibitor with an IC_{50} value of 39.6 ± 1.9. Its selectivity for the $P2Y_2$ receptor vs. this enzyme is at least 500-fold, similar to its selectivity vs. most of the P2Y receptors (Tables 1 and 4). However, in stark contrast is the observation that NPP1 does not discriminate between AR-C118925 and its de-methylated oxo-analog **5**. The methyl groups on the tricyclic substructure as well as the thiolactam

Table 1 Evaluation of AR-C118925 (**3**) and its derivatives **4** and **5** on different P2Y receptors

P2Y receptor	IC_{50} value (μM)[a] (or % inhibition at indicated concentration)		
	AR-C118925 (3)	Derivative 4	Derivative 5
Human $P2Y_1$ vs. ADP Ca^{2+} assay	**36.9** ± 2.7	n.d.	**>100** (30 % at 100 μM)
Human $P2Y_2$ vs. UTP Ca^{2+} assay	**0.0721** ± 0.0124	**5.45** ± 1.07	**≈100** (49 % at 100 μM)[b]
Human $P2Y_2$ vs. ATP Ca^{2+} assay	**0.0574** ± 0.0196	n.d.	n.d.
Human $P2Y_2$ vs. UTP β-arrestin assay	**0.716** ± 0.044	n.d.	**149** ± 14
Human $P2Y_2$ vs. AP_4A β-arrestin assay	**0.191** ± 0.024	n.d.	n.d.
Rat $P2Y_2$ vs. UTP Ca^{2+} assay	**0.291** ± 0.047	n.d.	**>>10** (0 % at 10 μM)
Human $P2Y_4$ vs. UTP Ca^{2+} assay	**37.1** ± 7.2	**9.42** ± 4.84	**≈100** (49 % at 100 μM)
Human $P2Y_6$ vs. UDP Ca^{2+} assay	**30.4** ± 3.1	n.d.	**>>100** (0 % at 100 μM)
Rat $P2Y_6$ vs. UDP Ca^{2+} assay	**>100** (13 % at 100 μM)	**≈100** (64 % at 100 μM)	**>100** (20 % at 100 μM)
Human $P2Y_{11}$ vs. ATP Ca^{2+} assay	**4.02** ± 0.73	n.d.	n.d.
Human $P2Y_{12}$ vs. 2-MeSATP β-arrestin assay	**33.7** ± 2.7	n.d.	n.d.
Human $P2Y_{14}$ vs. UDP-glucose β-arrestin assay	**>3** (26 % at 3 μM)	n.d.	n.d.

Mean IC50 values are presented in bold followed by SEM

n.d. not determined due to limited amount of compound available

[a] n = 3–8, unless stated otherwise. Receptor was activated with an agonist concentration that induced 80 % of maximal stimulation (EC_{80})

[b] n = 2

Table 2 Evaluation of AR-C118925 (**3**) and its derivative **5** on P2X receptors using the calcium mobilization assay

P2X receptor	IC_{50} value (μM)[a] (or % inhibition at indicated concentration)	
	AR-C118925 (**3**)	Derivative **5**
Human P2X1	**2.63** ± 0.49	**>10** (11 % at 10 μM)
Human P2X2	**>10** (22 % at 10 μM)	**>>10** (2 % at 10 μM)
Human P2X3	**0.819** ± 0.102	**7.45** ± 0.52
Human P2X4	**>>10** (4 % at 10 μM)	**>>10** (9 % at 10 μM)
Rat P2X4	**>>10** (2 % at 10 μM)	**>>10** (2 % at 10 μM)
Mouse P2X4	**>10** (14 % at 10 μM)	**>>10** (2 % at 10 μM)
Human P2X7	**>>10** (−26 % at 10 μM)	**>10** (−42 % at 10 μM)

Mean IC50 values are presented in bold followed by SEM

[a] n = 3–4. Receptor was activated with ATP at a concentration that induced 80 % of maximal stimulation (EC_{80})

group, therefore, do not appear to be involved in compound recognition. AR-C118925 (**3**) is only weakly potent or inactive on the human NPP2, NPP3, and the human nucleoside triphosphate diphosphohydrolases (NTPDase) 1, 2, 3, and 8 (Table 4). On the rat ecto-5′-nucleotidase (E5′-NT), AR-C118925 has a K_i value of 8.76 ± 2.80 μM. More data on the evaluation of AR-C118925 and its derivative **5** on other targets not directly related to purinergic signaling can be found in Table 1 of the Supporting information.

Mode of antagonism of AR-C118925 on the $P2Y_2$ receptor

In order to determine whether AR-C118925 acts as a competitive or an allosteric antagonist on the $P2Y_2$ receptor, we determined concentration-effect curves for the agonist UTP (**1b**) following pre-incubation with different, fixed concentrations of AR-C118925 using both the calcium mobilization assay (Fig. 5a) as well as the β-arrestin assay (Fig. 5b). In both assays, a clear parallel shift of the UTP curve towards higher UTP concentrations and an increasing EC_{50} value for UTP could be observed with increasing concentrations of AR-C118925 (**3**), while the upper plateaus of the curves remained approximately constant. The corresponding Schild plots both showed a linear curve with a slope close to 1 (0.816 for the calcium mobilization assay and 0.817 for the β-arrestin assay) and their x-axis intercepts, corresponding to the pA_2 value, were in the same range (37.2 nM in the calcium mobilization assay and 51.3 nM in the β-arrestin assay). The results from both in vitro assays correlate well with each other and provide strong evidence that the mode of antagonism of AR-C118925 (**3**) is competitive. This would also have been expected from the structure of AR-C118925 (**3**), which had been designed as an analog of the agonist UTP.

Physicochemical and pharmacokinetic properties of AR-C118925

To further characterize AR-C118925 (**3**) in terms of its physicochemical and pharmacokinetic properties, we sent it to a contract research organization (Pharmacelsus GmbH, Saarbrücken, Germany) for in vitro assessments on its absorption, distribution, metabolism, and excretion (ADME) properties. The semi-thermodynamic solubility, plasma protein binding, metabolic stability, cytochrome P450 enzyme inhibition, and permeability of Caco2 cell monolayers of the $P2Y_2$ antagonist were determined.

To assess its semi-thermodynamic solubility, 200 μM of AR-C118925 were dissolved in phosphate-buffered saline (PBS) containing 1 % DMSO. The mean concentration determined was 124 ± 12 μM (n = 3), indicating a relatively high solubility in PBS at pH 7.4. This is due to the acidic tetrazole moiety, which is deprotonated under physiological conditions. With respect to the plasma protein binding determination, 99 ± 0 % at 10 μM of

Table 3 Evaluation of AR-C118925 (**3**) and its derivative **5** on adenosine receptors using radioligand receptor binding assays

Receptor	K_i value (μM) (or % inhibition at indicated concentration)	
	AR-C118925 (3)	Derivative 5
Human adenosine A_1	**>>1** (1 % at 1 μM)[b]	**>>1** (−10 % at 1 μM)[b]
Human adenosine A_{2A}	**9.16** ± 1.57[a]	**>10** (17 % at 10 μM)[b]
Human adenosine A_{2B}	**>>1** (−4 % at 1 μM)[b]	**>1** (−43 % at 1 μM)[c]
Human adenosine A_3	**≥10** (44 % at 10 μM)[b]	**11.2** ± 2.3[a]

Mean IC50 values are presented in bold followed by SEM

[a] n = 3

[b] n = 2

[c] n = 1

Table 4 Evaluation of AR-C118925 (**3**) and its derivative **5** on ectonucleotidases

Enzyme	IC_{50} value (μM)[a] (or % inhibition at indicated concentration)	
	AR-C118925 (3)	Derivative 5
Human NPP1	**39.6** ± 1.9[b]	**39.7** ± 6.0
Human NPP2	**>100** (31 % at 100 μM)	n.d.
Human NPP3	**>100** (11 % at 100 μM)	n.d.
Human NTPDase 1	**>20** (10 % at 20 μM)	n.d.
Human NTPDase 2	**>20** (17 % at 20 μM)	**>>20** (0 % at 20 μM)[b]
Human NTPDase 3	**>20** (27 % at 20 μM)	n.d.
Human NTPDase 8	**>>20** (2 % at 20 μM)	n.d.
Rat E5′-NT	K_i = **8.76** ± 2.80	$K_i \approx$ **40**[c]

Mean IC50 values are presented in bold followed by SEM

n.d. not determined due to limited amount of compound available

[a] $n = 3$, unless stated otherwise

[b] $n = 2$

[c] $n = 1$

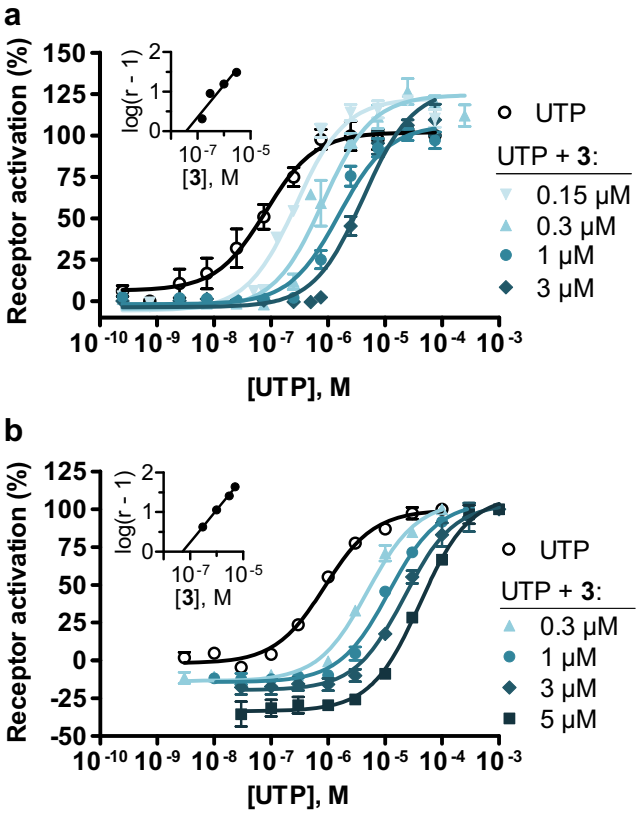

Fig. 5 Dose-response curves of UTP (**1b**) on the human $P2Y_2$ receptor following pre-incubation with different, fixed concentrations of AR-C118925 (**3**), determined using **a** the calcium mobilization assay and **b** the β-arrestin assay. Data points represent mean values ± SEM of three to six separate experiments performed in duplicates. Where no error bar is apparent, the SEM is too low to be visible. The *inserts* show the respective Schild plot: **a** slope = 0.816 and $pA_2 = pK_B = 10^{-7.43}$, corresponding to 37.2 nM. **b** Slope = 0.817 and $pA_2 = pK_B = 10^{-7.29}$, corresponding to 51.3 nM. The EC_{50} values and maximum receptor activation for (**a**) and (**b**) are shown in Tables 2 and 3 in the Supporting Information. *r* concentration ratio of the antagonist AR-C118925

AR-C118925 (**3**) in the presence of 2 % DMSO was measured. However, the recovery rate was very low (9 %), likely due to unspecific binding or instability in plasma. Furthermore, the susceptibility to metabolism in the liver was tested by incubation of 1 μM of AR-C118925 (**3**) with human and mouse liver microsomes and measuring the concentration of the remaining compound at different time points. Over the entire course of 1 h, the concentration of AR-C118925 (**3**) remained at approximately 1 μM and was, thus, not metabolized significantly (Fig. 1 in the Supporting information). These results show that AR-C118925 (**3**) appears to have a very high metabolic stability in humans as well as in mice, which is an important prerequisite for in vivo studies.

Cytochrome P450 (CYP) is an enzyme family that plays an important role in the metabolism of endogenous and exogenous compounds, including many drugs. Thus, it is undesirable for a compound to influence CYP activity. The ability of AR-C118925 (**3**) to inhibit nine CYP enzyme subtypes relevant for drug metabolism was assessed and results are summarized in Fig. 6. While several CYP subtypes were inhibited by AR-C118925 (**3**) at

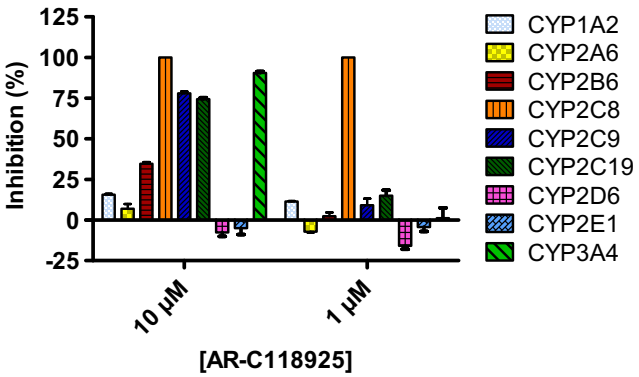

Fig. 6 Inhibition of human cytochrome P450 enzymes by AR-C118925. Data points represent mean values ± SEM of three separate experiments

higher concentrations of 10 μM, only CYP2C8 was inhibited at 1 μM to a significant extent. CYP2C8 is involved in the metabolism or bioactivation of several drugs, including, for example, the anti-cancer drug paclitaxel. [42].

Finally, the ability of AR-C118925 to permeate a monolayer of Caco2 cells was determined. This cell line was derived from a colon carcinoma but if cultured under appropriate conditions, it differentiates and expresses the phenotype of small intestine enterocytes [43]. Thus, Caco2 cell monolayers are widely used as in vitro models of the human small intestine mucosa to give an indication of the absorption properties following oral administration. We found that the permeability of AR-C118925 (**3**) was moderate, similar to that of the hydrophilic reference compound atenolol (refer to Table 4 of the Supporting information). Thus, intravenous injection is probably the most effective route of administration for this compound.

Conclusions

We developed an improved synthesis scheme for obtaining gram amounts of the $P2Y_2$ receptor antagonist AR-C118925, along with two of its derivatives. Furthermore, we comprehensively characterized this compound in vitro. AR-C118925 was assessed on a broad range of different targets related to the $P2Y_2$ receptor, including subtypes of the P2Y and P2X families, adenosine receptors, enzymes involved in nucleotide metabolism, and P2 receptor-related G protein-coupled receptors. We found that the potency of AR-C118925 is in the mid-nanomolar range on the $P2Y_2$ receptor and that it is at least 400-fold selective for the $P2Y_2$ receptor vs. its structurally and pharmacologically closest relatives, the $P2Y_1$, $P2Y_4$, and $P2Y_6$ subtypes, as well as most other P2 and adenosine receptors, and selected ectonucleotidases. Lower selectivity was observed vs. the $P2Y_{11}$, P2X1, and P2X3 receptors (14- to 50-fold). Additionally, we determined the binding mode of AR-C118925 on the $P2Y_2$ receptor and obtained evidence for competitive antagonism. We deployed two different in vitro assays for our assessments: a calcium mobilization and a β-arrestin assay. The potency for AR-C118925 was in a similar range for both. Therefore, AR-C118925 appears to block the G_q-mediated, calcium-releasing pathway and β-arrestin recruitment to a similar extent. Finally, we provide data showing that AR-C118925 is well soluble in phosphate-buffered saline, has a very high metabolic stability in liver microsomes, inhibits CYP2C8 but not eight other CYP enzymes at 1 μM, and does not permeate Caco2 cell monolayers to a large extent. Owing to the scarcity of selective antagonists for most P2Y receptors and the $P2Y_2$ receptor in particular, AR-C118925 is undoubtedly useful as a pharmacological tool to study $P2Y_2$ receptor functions. The described synthetic procedure will facilitate access to this $P2Y_2$ receptor antagonist by other research groups, including larger amounts for structural and in vitro studies.

Acknowledgments This study was supported by the Ministry for Innovation, Science, Research and Technology of the State of North Rhine-Westphalia through the NRW International Graduate Research School Biotech-Pharma (M.R., C.E.M.). We thank Amelie Fiene, Angelika Fischer, Marianne Freundlieb, Sonja Hinz, Sangyong Lee, Anika Püsche, Anja B. Scheiff, Clara B. Schoeder, and Stefanie Weyer for selectivity testing.

Compliance with ethical standards

Conflict of interest The authors declare that there is no conflict of interest.

References

1. Abbracchio MP, Burnstock G, Boeynaems JM, Barnard EA, Boyer JL, Kennedy C, Knight GE, Fumagalli M, Gachet C, Jacobson KA, Weisman GA (2006) International Union of Pharmacology LVIII: update on the P2Y G protein-coupled nucleotide receptors: from molecular mechanisms and pathophysiology to therapy. Pharmacol Rev 58:281–341
2. Lustig KD, Shiau AK, Brake AJ, Julius D (1993) Expression cloning of an ATP receptor from mouse neuroblastoma cells. Proc Natl Acad Sci U S A 90:5113–5117
3. Murthy KS, Makhlouf GM (1998) Coexpression of ligand-gated P2X and G protein-coupled P2Y receptors in smooth muscle. Preferential activation of P2Y receptors coupled to phospholipase C (PLC)-beta1 via Galphaq/11 and to PLC-beta3 via Gbetagammai3. J Biol Chem 273:4695–4704
4. Bagchi S, Liao Z, Gonzalez FA, Chorna NE, Seye CI, Weisman GA, Erb L (2005) The P2Y2 nucleotide receptor interacts with alphav integrins to activate go and induce cell migration. J Biol Chem 280:39050–39057
5. Liao Z, Seye CI, Weisman GA, Erb L (2007) The P2Y2 nucleotide receptor requires interaction with alpha v integrins to access and activate G12. J Cell Sci 120:1654–1662
6. Baltensperger K, Porzig H (1997) The P2U purinoceptor obligatorily engages the heterotrimeric G protein G16 to mobilize intracellular Ca2+ in human erythroleukemia cells. J Biol Chem 272: 10151–10159
7. Moore DJ, Chambers JK, Wahlin JP, Tan KB, Moore GB, Jenkins O, Emson PC, Murdock PR (2001) Expression pattern of human P2Y receptor subtypes: a quantitative reverse transcription-polymerase chain reaction study. Biochim Biophys Acta 1521: 107–119
8. Cressman VL, Lazarowski E, Homolya L, Boucher RC, Koller BH, Grubb BR (1999) Effect of loss of P2Y(2) receptor gene expression on nucleotide regulation of murine epithelial Cl(−) transport. J Biol Chem 274:26461–26468
9. Hochhauser E, Cohen R, Waldman M, Maksin A, Isak A, Aravot D, Jayasekara PS, Müller CE, Jacobson KA, Shainberg A (2013) P2Y receptor agonist with enhanced stability protects the heart from ischemic damage in vitro and in vivo. Purinergic Signal 9: 633–642
10. Camden JM, Schrader AM, Camden RE, Gonzalez FA, Erb L, Seye CI, Weisman GA (2005) P2Y2 nucleotide receptors enhance alpha-secretase-dependent amyloid precursor protein processing. J Biol Chem 280:18696–18702
11. Xing M, Post S, Ostrom RS, Samardzija M, Insel PA (1999) Inhibition of phospholipase A2-mediated arachidonic acid release by cyclic AMP defines a negative feedback loop for P2Y receptor

activation in Madin-Darby canine kidney D1 cells. J Biol Chem 274:10035–10038
12. Xu J, Weng YI, Simonyi A, Krugh BW, Liao Z, Weisman GA, Sun GY (2002) Role of PKC and MAPK in cytosolic PLA2 phosphorylation and arachadonic acid release in primary murine astrocytes. J Neurochem 83:259–270
13. Xu J, Chalimoniuk M, Shu Y, Simonyi A, Sun AY, Gonzalez FA, Weisman GA, Wood WG, Sun GY (2003) Prostaglandin E2 production in astrocytes: regulation by cytokines, extracellular ATP, and oxidative agents. Prostaglandins Leukot Essent Fatty Acids 69:437–448
14. Welch BD, Carlson NG, Shi H, Myatt L, Kishore BK (2003) P2Y2 receptor-stimulated release of prostaglandin E2 by rat inner medullary collecting duct preparations. Am J Physiol Renal Physiol 285: F711–F721
15. Seye CI, Kong Q, Erb L, Garrad RC, Krugh B, Wang M, Turner JT, Sturek M, Gonzalez FA, Weisman GA (2002) Functional P2Y2 nucleotide receptors mediate uridine 5′-triphosphate-induced intimal hyperplasia in collared rabbit carotid arteries. Circulation 106: 2720–2726
16. Schumacher D, Strilic B, Sivaraj KK, Wettschureck N, Offermanns S (2013) Platelet-derived nucleotides promote tumor-cell transendothelial migration and metastasis via P2Y2 receptor. Cancer Cell 24:130–137
17. Wilden PA, Agazie YM, Kaufman R, Halenda SP (1998) ATP-stimulated smooth muscle cell proliferation requires independent ERK and PI3K signaling pathways. Am J Phys 275:H1209–H1215
18. Tu MT, Luo SF, Wang CC, Chien CS, Chiu CT, Lin CC, Yang CM (2000) P2Y(2) receptor-mediated proliferation of C(6) glioma cells via activation of Ras/Raf/MEK/MAPK pathway. Br J Pharmacol 129:1481–1489
19. Muscella A, Elia MG, Greco S, Storelli C, Marsigliante S (2003) Activation of P2Y2 receptor induces c-FOS protein through a pathway involving mitogen-activated protein kinases and phosphoinositide 3-kinases in HeLa cells. J Cell Physiol 195:234–240
20. Schafer R, Sedehizade F, Welte T, Reiser G (2003) ATP- and UTP-activated P2Y receptors differently regulate proliferation of human lung epithelial tumor cells. Am J Physiol Lung Cell Mol Physiol 285:L376–L385
21. Greig AV, Linge C, Cambrey A, Burnstock G (2003) Purinergic receptors are part of a signaling system for keratinocyte proliferation, differentiation, and apoptosis in human fetal epidermis. J Invest Dermatol 121:1145–1149
22. Malam-Souley R, Seye C, Gadeau AP, Loirand G, Pillois X, Campan M, Pacaud P, Desgranges C (1996) Nucleotide receptor P2u partially mediates ATP-induced cell cycle progression of aortic smooth muscle cells. J Cell Physiol 166:57–65
23. Miyagi Y, Kobayashi S, Ahmed A, Nishimura J, Fukui M, Kanaide H (1996) P2U purinergic activation leads to the cell cycle progression from the G1 to the S and M phases but not from the G0 to G1 phase in vascular smooth muscle cells in primary culture. Biochem Biophys Res Commun 222:652–658
24. Kishore BK, Carlson NG, Ecelbarger CM, Kohan DE, Müller CE, Nelson RD, Peti-Peterdi J, Zhang Y (2015) Targeting renal purinergic signalling for the treatment of lithium-induced nephrogenic diabetes insipidus. Acta Physiol 214:176–188
25. Hoebertz A, Mahendran S, Burnstock G, Arnett TR (2002) ATP and UTP at low concentrations strongly inhibit bone formation by osteoblasts: a novel role for the P2Y2 receptor in bone remodeling. J Cell Biochem 86:413–419
26. Brunschweiger A, Müller CE (2006) P2 receptors activated by uracil nucleotides—an update. Curr Med Chem 12:763–771
27. Kemp PA, Sugar RA, Jackson AD (2004) Nucleotide-mediated mucin secretion from differentiated human bronchial epithelial cells. Am J Respir Cell Mol Biol 31:446–455
28. Meghani P (2002) The design of P2Y2 antagonists for the treatment of inflammatory diseases. American Chemical Society Division of Medicinal Chemistry Abstracts of 224th ACS National Meeting
29. Cosentino S, Banfi C, Burbiel JC, Luo H, Tremoli E, Abbracchio MP (2012) Cardiomyocyte death induced by ischaemic/hypoxic stress is differentially affected by distinct purinergic P2 receptors. J Cell Mol Med 16:1074–1084
30. Önnheim K, Christenson K, Gabl M, Burbiel JC, Müller CE, Oprea TI, Bylund J, Dahlgren C, Forsman H (2014) A novel receptor cross-talk between the ATP receptor P2Y2 and formyl peptide receptors reactivates desensitized neutrophils to produce superoxide. Exp Cell Res 323:209–217
31. Wang S, Iring A, Strilic B, Albarrán Juárez J, Kaur H, Troidl K, Tonack S, Burbiel JC, Müller CE, Fleming I, Lundberg JO, Wettschureck N, Offermanns S (2015) $P2Y_2$ and Gq/G_{11} control blood pressure by mediating endothelial mechanotransduction. J Clin Invest 125:3077–3086
32. Hilbert G, Jansen E (1934) Action of alkali and ammonia on 2,4-dialkoxypyrimidines. JACS 56:134–139
33. Whittaker N (1953) Notes J Chem Soc:1646
34. Wheeler HL, Bristol HS (1905) Amer Chem J 32:437
35. Kindon N, Meghani P, Thom S (1998) Novel Compounds. WO1998054180
36. Knight D, Nott A (1981) The generation and chemistry of dianions derived from furancarboxylic acids. J Chem Soc 1125–1131
37. Hillmann P, Ko GY, Spinrath A, Raulf A, von Kügelgen I, Wolff SC, Nicholas RA, Kostenis E, Holtje HD, Müller CE (2009) Key determinants of nucleotide-activated G protein-coupled P2Y(2) receptor function revealed by chemical and pharmacological experiments, mutagenesis and homology modeling. J Med Chem 52: 2762–2775
38. Hernandez-Olmos V, Abdelrahman A, El-Tayeb A, Freudendahl D, Weinhausen S, Müller CE (2012) N-substituted phenoxazine and acridone derivatives: structure–activity relationships of potent P2X4 receptor antagonists. J Med Chem 55:9576–9588
39. Fuchs A, Rempel V, Müller CE (2013) The natural product magnolol as a lead structure for the development of potent cannabinoid receptor agonists. PLoS One 8:e77739
40. Burbiel J (2006) On the syntheses of dibenzosuberenone and 2,8-dimethyldibenzosuberenone. ARKIVOC xiii:16–21
41. Wild H, Hansen J, Lautz J, Paessens A (1993) 5-Oxo-dibenzo[a, d]cyclohepta-1,4-dienes and their use as retroviral agents. Eur Pat 0589322:A1
42. Vaclavikova R, Horsky S, Simek P, Gut I (2003) Paclitaxel metabolism in rat and human liver microsomes is inhibited by phenolic antioxidants. Naunyn Schmiedeberg's Arch Pharmacol 368:200–209
43. Hidalgo IJ, Raub TJ, Borchardt RT (1989) Characterization of the human colon carcinoma cell line (Caco-2) as a model system for intestinal epithelial permeability. Gastroenterology 96:736–749